Paper 221

Proceedings of the Eleventh International Conference
on Computational Structures Technology,
B.H.V. Topping, (Editor),
Civil-Comp Press, Stirlingshire, Scotland

Isogeometric Shell Formulation based on a Classical Shell Model

A.H. Niemi[1], N. Collier[1], L. Dalcin[2], M. Ghommem[2] and V.M. Calo[1]
[1] King Abdullah University of Science and Technology (KAUST)
Thuwal, Kingdom of Saudi Arabia
[2] Consejo Nacional de Investigaciones Científicas y Técnicas
Santa Fe, Argentina

Abstract

We study a Reissner-Mindlin shell formulation for NURBS-based isogeometric analysis. The formulation is based on a shell model which utilizes curvilinear coordinates and analytic integration thorough the thickness. We examine the accuracy of the approach in the pinched cylinder benchmark problem and present comparisons against the h-version of FEM with bilinear elements. The analysis is performed with the `PetIGA` and `igakit` software packages.

Keywords: isogeometric analysis, shells, NURBS, benchmark study.

1 Introduction

Isogeometric analysis is a generalization of standard finite element analysis and was introduced by Hughes and collaborators in [1]. It aims at the integration of engineering design and analysis processes by using the functions commonly used for geometry representation in computer aided design (CAD) as a basis for finite element analysis. These functions include non-uniform rational B-splines (NURBS) and their recent generalization, T-splines, see [2]. Isogeometric analysis *fits like a glove* to shell structures since representation of surfaces is well established in computer graphics and shell geometries are often described in terms of the middle surface and its normal vector.

The present study constitutes the first steps in our work concerning isogeometric shell analysis. We introduce an isogeometric shell model of Reissner-Mindlin type and study its accuracy in the classical pinched cylinder benchmark problem. Our formulation is based on shell model where the displacement, strain and stress fields are defined in terms of a curvilinear coordinate system arising from the NURBS description of the shell middle surface. It should be noted that splines have been employed earlier in shell analysis in the works [1, 2, 3, 4, 5] but also other techniques such as subdivision surfaces have been used to fuse geometry with analysis, see [6, 7].

Our isogeometric shell formulation is implemented using the `PetIGA` and `igakit` software packages developed by Collier and Dalcin. The `igakit` package is a Python package used to generate NURBS representations of geometries that can be utilized by the `PetIGA` finite element framework. The latter utilises data structures and routines of the Portable, Extensible Toolkit for Scientific Computation (`PETSc`), see [8, 9]. Our current shell implementation is valid for static, linear problems only, but the software package is well suited for future extensions to geometrically and materially nonlinear regime as well as to dynamic problems.

The paper is structured as follows. We outline the fundamentals of NURBS-based isogeometric analysis in Section 2. The Reissner-Mindlin shell formulation is presented in Section 3. In Section 4 we use the formulation to solve the popular pinched cylinder benchmark problem and compare the results with the ones obtained by using the h-version of FEM and bilinear elements. Conclusions and future research directions are presented in Section 5.

2 Isogeometric Analysis using NURBS

In this section we present a summary of representation of surfaces using NURBS and the related finite element analysis. For more detailed discussion, see for instance [10, 11, 12].

2.1 B-spline curves

B-splines are piecewise polynomial curves defined in terms of B-spline basis functions. The basis functions of degree p, denoted by $N_{i,p}(\xi)$, associated to a non-decreasing set of coordinates called the knot vector $\mathcal{X} = \{\xi_1, \xi_2, \ldots, \xi_{n+p+1}\}$ are defined recursively as

$$
\begin{aligned}
N_{i,0}(\xi) &= \begin{cases} 1, & \xi_i \le \xi < \xi_{i+1} \\ 0, & \text{otherwise} \end{cases} \\
N_{i,p}(\xi) &= \frac{\xi - \xi_i}{\xi_{i+p} - \xi_i} N_{i,p-1}(\xi) + \frac{\xi_{i+p+1} - \xi}{\xi_{i+p+1} - \xi_{i+1}} N_{i+1,p-1}(\xi), \quad p > 0
\end{aligned}
\tag{1}
$$

for $i = 1, \ldots, n$ and $p \ge 1$. A B-spline basis function is C^∞ between two distinct knots and C^{p-1} at a single knot. If a knot is repeated in the knot vector k times then the continuity is C^{p-k} at that knot. Consequently, the basis becomes interpolatory at knots with multiplicity p whereas knot multiplicity of $p+1$ makes the basis discontinuous and is used at the end points to make the knot vector open.

The B-spline curve of degree p with control points $\mathbf{P}_1, \ldots, \mathbf{P}_n$ is defined on the interval $[a, b] = [\xi_{p+1}, \xi_{n+1}]$ as the linear combination of the control points and basis functions

$$\mathbf{C}(\xi) = \sum_{i=1}^{n} N_{i,p}(\xi)\mathbf{P}_i$$

We recall that the piecewise linear interpolation of the control points is called the control polygon. For open knot vectors, the B-spline curve interpolates the first and last control points and is tangential to the control polygon at these points.

2.2 B-spline surfaces

A B-spline surface is defined using tensor products of B-spline basis functions written in two parametric coordinates ξ, η. If $N_{i,p}$ and $M_{j,q}$ denote basis functions of degree p and q associated to the knot vectors $\mathcal{X} = \{\xi_1, \xi_2, \ldots, \xi_{n+p+1}\}$ and $\mathcal{Y} = \{\eta_1, \eta_2, \ldots, \eta_{m+q+1}\}$ and $\mathbf{P}_{ij}$, $i = 1, \ldots, n$, $j = 1, \ldots, m$ is a net of control points in 3-space, the B-spline surface is defined as

$$\mathbf{S}(\xi, \eta) = \sum_{i=1}^{n} \sum_{j=1}^{m} N_{i,p}(\xi) M_{j,q}(\eta) \mathbf{P}_{ij}$$

For open knot vectors, the surface interpolates the control net at the vertices.

2.3 NURBS

Non-uniform Rational B-Splines (NURBS) are obtained from integral B-splines by supplementing each control point with a scalar weight. The NURBS curve of degree p with control points $\mathbf{P}_i$ is defined as

$$\mathbf{C}(\xi) = \frac{\sum_{i=1}^{n} N_{i,p}(\xi) w_i \mathbf{P}_i}{\sum_{i=1}^{n} N_{i,p}(\xi) w_i}$$

where $N_{i,p}(\xi)$ are the B-spline basis functions defined by (1). The curve can also be written in the form

$$\mathbf{C}(\xi) = \sum_{i=1}^{n} R_{i,p}(\xi)\mathbf{P}_i$$

where

$$R_{i,p}(\xi) = \frac{w_i N_{i,p}(\xi)}{\sum_{j=1}^{n} w_j N_{j,p}(\xi)}$$

stand for the rational B-spline basis functions.

It should be noted that the weights define the control points in homogeneous coordinates as $\hat{\mathbf{P}}_i = (w_i x_i, w_i y_i, w_i z_i, w_i)$ and that in homogeneous coordinates a NURBS curve has the form

$$\mathbf{C}(\xi) = \sum_{i=1}^{n} N_{i,p}(\xi)\hat{\mathbf{P}}_i$$

and allow the representation of hyberbolas and ellipses.

Similarly a NURBS surface has the representation

$$\mathbf{S}(\xi,\eta) = \frac{\sum_{i=1}^{n}\sum_{j=1}^{m} N_{i,p}(\xi)M_{j,q}(\eta)w_{ij}\mathbf{P}_{ij}}{\sum_{i=1}^{n}\sum_{j=1}^{m} N_{i,p}(\xi)M_{j,q}(\eta)w_{ij}}$$

where the control point net $\mathbf{P}_{ij}$ is augmented with the weights w_{ij} for $i = 1,\ldots,n$ and $j = 1,\ldots,m$.

2.4 Finite Element Analysis using NURBS

The isogeometric finite element method is obtained from the exact geometry representation by invoking the isoparametric concept, that is, by using the same basis functions used to represent the geometry to approximate the unknown function. The two basic mechanisms for controlling the accuracy of the approximation in isogeometric analysis are knot insertion and degree elevation. The idea is to enrich the NURBS basis without changing the surface geometrically or parametrically. This can be achieved by changing the number and location of the control points in a suitable way, see [12] for more details. Both refinement techniques are implemented in the `igakit` package.

3 Isogeometric Shell Formulation

3.1 The Principle of Virtual Work

The starting point of our formulation is the principle of virtual work written in the abstract form as

$$\text{Find } \mathbf{u} \in \mathcal{U} \text{ s.t.} \quad \mathcal{A}(\mathbf{w},\mathbf{u}) = \mathcal{L}(\mathbf{w}) \quad \forall \mathbf{w} \in \mathcal{U}_0 \tag{2}$$

where $\mathbf{u}$ is the displacement field, $\mathcal{A}$ is a bilinear form representing the virtual work associated to the virtual displacement field $\mathbf{w}$ and $\mathcal{L}$ is a linear functional returning the potential energy of the external loads. The energy space $\mathcal{U}$ consists of kinematically admissible displacement fields for which the strain energy $\mathcal{A}(\mathbf{u},\mathbf{u})$ is finite and $\mathcal{U}_0$ is the same energy space where the possible kinematic constraints are taken to be homogeneous.

For an elastic body occupying a three-dimensional domain Ω the virtual work can be expressed in terms of the stress tensor $\boldsymbol{\sigma}$ and the strain tensor $\boldsymbol{\varepsilon}$ as

$$\mathcal{A}(\mathbf{w},\mathbf{u}) = \int_\Omega \boldsymbol{\varepsilon}(\mathbf{w}) : \boldsymbol{\sigma}(\mathbf{u})\, \mathrm{d}\Omega \tag{3}$$

When the domain Ω is thin, that is, one of its dimensions is small as compared with the other two, it is possible to simplify (2) by making assumptions concerning the form of the displacement and stress fields in the thin direction. The formal procedure for linearly elastic shells is outlined next.

3.2 Dimensionally Reduced Shell Model

A shell domain is defined as $\Omega = \mathbf{\Phi}(\hat{\Omega} \times (-t/2, t/2))$, where the map $\mathbf{\Phi}$ is of the form

$$\mathbf{\Phi}(\xi, \eta, \zeta) = \mathbf{S}(\xi, \eta) + \zeta \mathbf{n}(\xi, \eta)$$

Here $\mathbf{S}(\xi, \eta)$ refers to the NURBS description of the middle surface and $\mathbf{n}(\xi, \eta)$ stands for the unit normal vector to the middle surface. Without losing any generality we may set $\hat{\Omega} = (0, 1) \times (0, 1)$.

We make the following simplifying assumptions regarding the deformation of a shell body:

1. Normal fibres to the middle surface remain straight

2. Normal fibres do not stretch

3. The transverse normal stress is negligible

Denoting the tangential displacements along the coordinate lines ξ, η by U_1, U_2, and the normal displacement by U_3, the above kinematic assumptions can be imposed by writing

$$\begin{aligned} U_1(\xi, \eta, \zeta) &= u(\xi, \eta) - \zeta\theta(\xi, \eta) \\ U_2(\xi, \eta, \zeta) &= v(\xi, \eta) - \zeta\psi(\xi, \eta) \\ U_3(\xi, \eta, \zeta) &= w(\xi, \eta) \end{aligned} \tag{4}$$

The generalized displacement field $\mathbf{u} = (u, v, w, \theta, \psi)$ in (4) consists of the tangential displacements (u, v) and the transverse deflection (w) of the middle surface, and of the rotations (θ, ψ) of the normal. The deformation can be described in terms of the membrane strains β_{ij}, transverse shear strains ρ_i, and bending strains κ_{ij} defined along the shell middle surface such that

$$\begin{aligned} \varepsilon_{ij} &= \beta_{ij} - z\kappa_{ij}, \quad & i, j = 1, 2 \\ 2\varepsilon_{i3} &= \rho_i, & i = 1, 2 \end{aligned}$$

Assuming that ξ, η are the (orthogonal) principal curvature coordinates associated with the principal curvatures b_1, b_2 and the metric parameters A_1, A_2, the strain fields take the form

$$
\begin{aligned}
\beta_{11} &= \frac{1}{A_1}\frac{\partial u}{\partial \xi} + \frac{1}{A_1 A_2}\frac{\partial A_1}{\partial \eta} v + b_1 w, \\
\beta_{22} &= \frac{1}{A_2}\frac{\partial v}{\partial \eta} + \frac{1}{A_1 A_2}\frac{\partial A_2}{\partial \xi} u + b_2 w, \\
\beta_{12} &= \frac{1}{2}\left(\frac{1}{A_2}\frac{\partial u}{\partial \eta} + \frac{1}{A_1}\frac{\partial v}{\partial \xi} - \frac{1}{A_1 A_2}\frac{\partial A_1}{\partial \eta} u - \frac{1}{A_1 A_2}\frac{\partial A_2}{\partial \xi} v\right), \\
\rho_1 &= \theta - \frac{1}{A_1}\frac{\partial w}{\partial \xi} + b_1 u, \\
\rho_2 &= \psi - \frac{1}{A_2}\frac{\partial w}{\partial \eta} + b_2 v, \\
\kappa_{11} &= \frac{1}{A_1}\frac{\partial \theta}{\partial \xi} + \frac{1}{A_1 A_2}\frac{\partial A_1}{\partial \eta}\psi, \\
\kappa_{22} &= \frac{1}{A_2}\frac{\partial \psi}{\partial \eta} + \frac{1}{A_1 A_2}\frac{\partial A_2}{\partial \xi}\theta, \\
\kappa_{12} &= \frac{1}{2}\left[\frac{1}{A_2}\frac{\partial \theta}{\partial \eta} + \frac{1}{A_1}\frac{\partial \psi}{\partial \xi} - \frac{1}{A_1 A_2}\frac{\partial A_1}{\partial \eta}\theta - \frac{1}{A_1 A_2}\frac{\partial A_2}{\partial \xi}\psi\right. \\
&\quad \left. -b_1\left(\frac{1}{A_2}\frac{\partial u}{\partial \eta} - \frac{1}{A_1 A_2}\frac{\partial A_2}{\partial \xi} v\right) - b_2\left(\frac{1}{A_1}\frac{\partial v}{\partial \xi} - \frac{1}{A_1 A_2}\frac{\partial A_1}{\partial \eta} u\right)\right].
\end{aligned} \tag{5}
$$

The above strain expressions agree with the expressions derived by Novozhilov in [13] under the assumptions

$$
\theta = \frac{1}{A_1}\frac{\partial w}{\partial x} - b_1 u, \quad \psi = \frac{1}{A_2}\frac{\partial w}{\partial y} - b_2 v.
$$

The strain expressions (5) were also used in [14] to study effect of mesh distortion to the accuracy of isoparametric FEM discretizations. Notice that in shell theory, different definitions of the bending strains are encountered. However, these differences are usually insignificant as compared with the initial assumptions of the theory.

The geometric parameters needed to evaluate (5) can be computed from the spline representation of the middle surface as

$$
\begin{aligned}
A_1 &= \left|\frac{\partial \mathbf{S}}{\partial \xi}\right|, & A_2 &= \left|\frac{\partial \mathbf{S}}{\partial \eta}\right| \\
b_1 &= -\frac{1}{A_1^2}\mathbf{n}\cdot\frac{\partial^2 \mathbf{S}}{\partial \xi^2}, & b_2 &= -\frac{1}{A_2^2}\mathbf{n}\cdot\frac{\partial^2 \mathbf{S}}{\partial \eta^2}
\end{aligned} \tag{6}
$$

and the unit normal can be computed as

$$
\mathbf{n} = \frac{\dfrac{\partial \mathbf{S}}{\partial \xi} \times \dfrac{\partial \mathbf{S}}{\partial \eta}}{\left|\dfrac{\partial \mathbf{S}}{\partial \xi} \times \dfrac{\partial \mathbf{S}}{\partial \eta}\right|} \tag{7}
$$

For homogeneous, isotropic linearly elastic material, the bilinear form (3) can be written approximatively as

$$\mathcal{A}(\mathbf{w},\mathbf{u}) = \int_{\hat{\Omega}} [\boldsymbol{\beta}(\mathbf{w}) : \mathbf{N}(\mathbf{u}) + \boldsymbol{\rho}(\mathbf{w}) \cdot \mathbf{V}(\mathbf{u}) + \kappa(\mathbf{w}) : \mathbf{M}(\mathbf{u})] \; A_1 A_2 \, \mathrm{d}\xi \mathrm{d}\eta \tag{8}$$

where the stress resultants are defined as

$$\begin{aligned}
\mathbf{N} &= \frac{Et}{1-\nu^2}[\nu \operatorname{tr}(\boldsymbol{\beta})\mathbf{I} + (1-\nu)\boldsymbol{\beta}] \\
\mathbf{V} &= \frac{Et}{2(1+\nu)}\boldsymbol{\rho} \\
\mathbf{M} &= \frac{Et^3}{12(1-\nu^2)}[\nu \operatorname{tr}(\boldsymbol{\kappa})\mathbf{I} + (1-\nu)\boldsymbol{\kappa}]
\end{aligned} \tag{9}$$

Equations (5)–(9) complete the description of our NURBS-based shell model. Notice that for smooth surfaces the finite strain energy condition $\mathcal{A}(\mathbf{u},\mathbf{u}) < \infty$ translates to the requirement that the first order partial derivatives of all displacement components in $\mathbf{u}$ are square integrable over $\hat{\Omega}$. This is in turn guaranteed because the NURBS basis functions are piecewise smooth and at least continuous.

4 Numerical Results

We consider as an example a pinched cylinder with end diaphragms which is one of the most popular benchmark problems in shell analysis. The initial geometry consists of a circular cylinder of radius $R = 100$ and length $2L = 100$. The cylinder is loaded by two normal point loads of magnitude $F = 1$ located centrally at the opposite sides of the cylinder. The material parameters are taken to be $E = 3 \cdot 10^7$ and $\nu = 0.3$.

By symmetry, it is sufficient to analyze only one eight of the cylinder. The geometry can represented using a single quadratic rational NURBS element associated to the knot vectors

$$\begin{aligned}
\mathcal{X} &= \{0,0,1,1\} \\
\mathcal{Y} &= \{0,0,0,1,1,1\}
\end{aligned}$$

and the control point net (written in homogeneous coordinates)

$$\hat{\mathbf{P}} = \begin{bmatrix} (0,-100,0,1) & \mu \cdot (0,-100,100,1) & (0,0,100,1) \\ (100,-100,0,1) & \mu \cdot (100,-100,100,1) & (100,0,100,1) \end{bmatrix}$$

where $\mu = \sqrt{2}/2$.

Figures 2 and 3 show convergence of the displacement under the load application point when $R/t = 100$ and $R/t = 1000$, respectively. Quadratic, cubic and quartic NURBS discretizations are compared against the isoparametric bilinear discretization introduced in [15]. However, this comparison is not completely fair since the variational formulation of the bilinear MITC4S formulation uses highly tuned strain

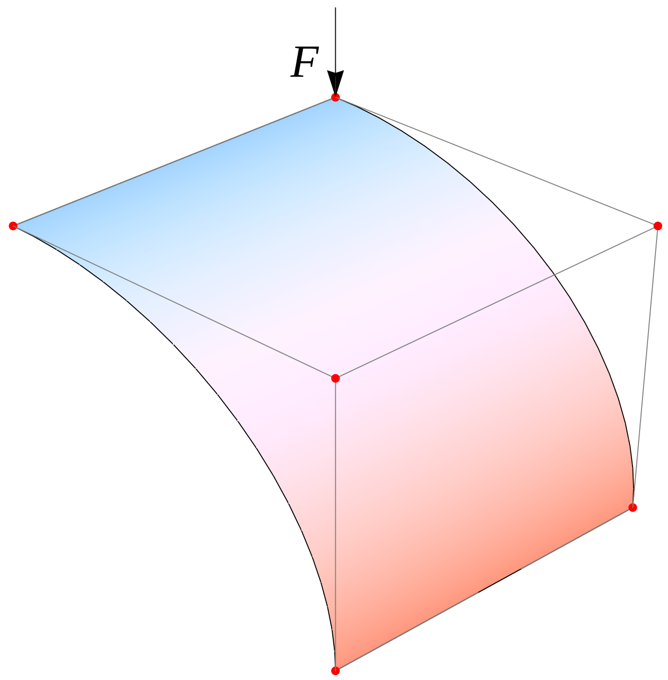

Figure 1: Initial geometry for the pinched cylinder problem.

expressions so as to avoid all parametric locking effects arising for small values of the thickness. The formulation also takes into account the geometric curvature of the shell inside each element which guarantees excellent coarse-mesh accuracy. In our NURBS formulation the geometry is always represented exactly but no attempt, other than increasing the approximation order, is made to avoid locking. Our results show that the quadratic and cubic NURBS approximations exhibit notably slower convergence under uniform knot insertion as the thickness decreases but the quartic approximation converges relatively quickly. It should be noted that in the current problem the deformation becomes rather localized around the load application point as the thickness decreases so that more h-refinement is required to achieve the same accuracy, see Figures 4 and 5.

5 Concluding Remarks

We have presented an isogeometric shell formulation utilizing NURBS. Our formulation is based on a dimensionally reduced shell model and its accuracy has been verified in the pinched cylinder benchmark problem. We have confirmed that higher-order NURBS provide good approximations within the standard variational framework.

Our future work is concerned with building an isogeometric model for nonlinear structural response of thin-walled shells undergoing large rigid-body motions. The aim is to use the model in a aeroelastic framework for the simulation of flapping wings.

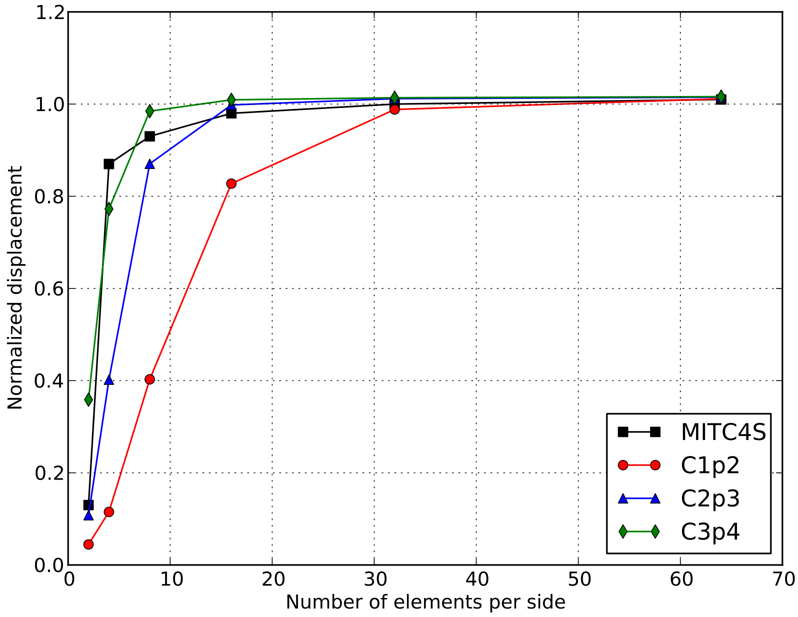

Figure 2: Strain energy convergence of the pinched cylindrical shell at $R/t = 100$. NURBS-based discretizations with maximal continuity vs. bilinear h-FEM.

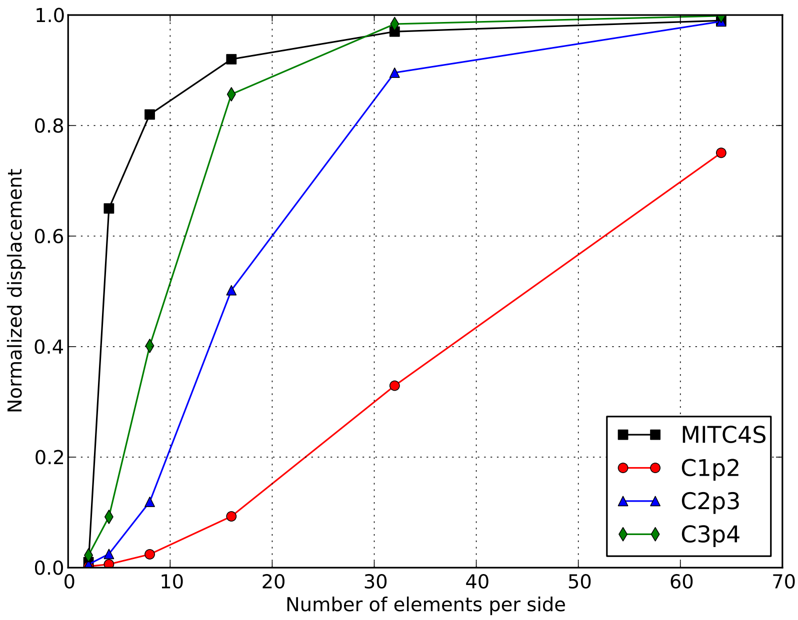

Figure 3: Strain energy convergence of the pinched cylindrical shell at $R/t = 1000$. NURBS-based discretizations with maximal continuity vs. bilinear h-FEM.

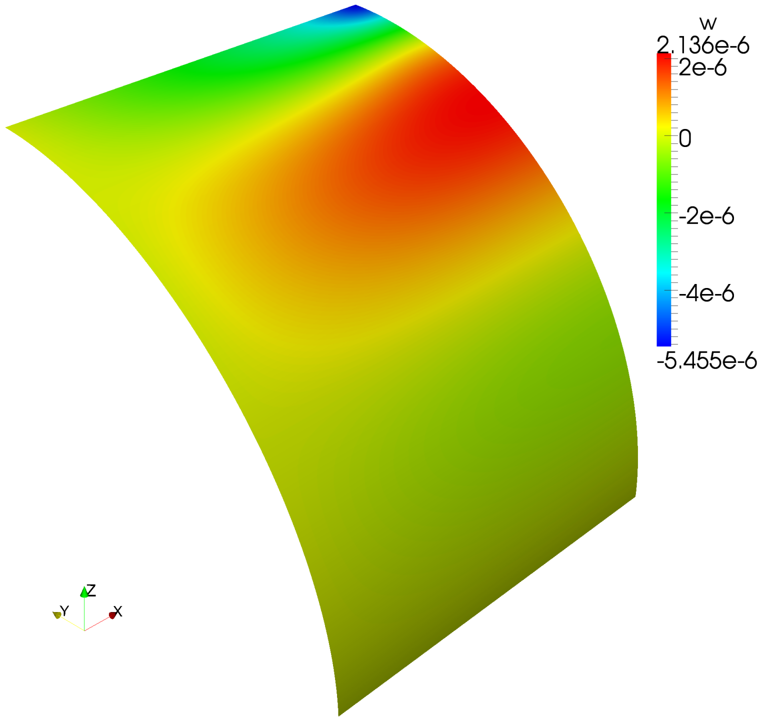

Figure 4: The transverse deflection of the pinched cylindrical shell at $R/t = 100$. Discretization with quartic NURBS with maximal continuity on 32×32 mesh.

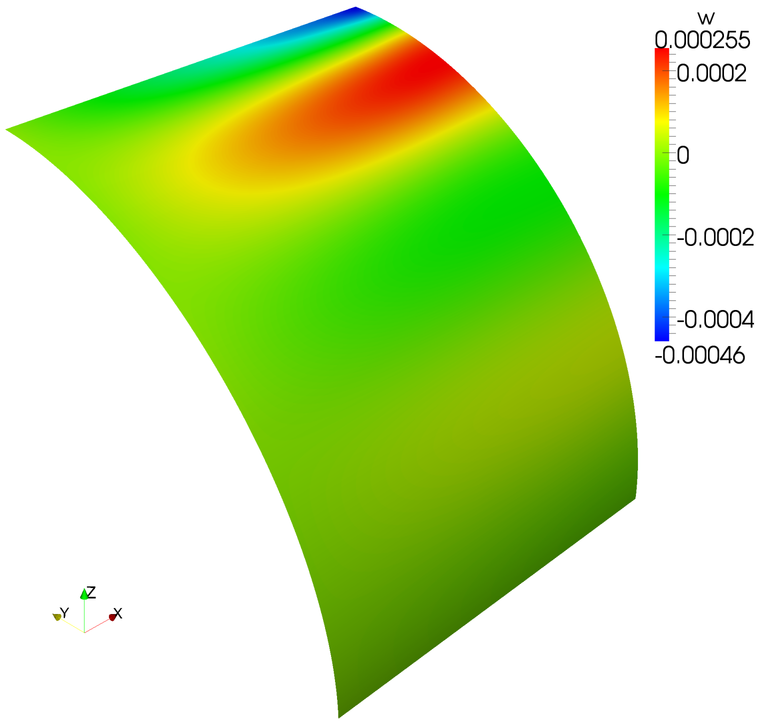

Figure 5: The transverse deflection of the pinched cylindrical shell at $R/t = 1000$. Discretization with quartic NURBS with maximal continuity on 32×32 mesh.

References

[1] T. Hughes, J. Cottrell, Y. Bazilevs, “Isogeometric analysis: CAD, finite elements, NURBS, exact geometry and mesh refinement”, *Computer Methods in Applied Mechanics and Engineering*, 194(39-41): 4135–4195, Oct. 2005, ISSN 00457825, URL `http://dx.doi.org/10.1016/j.cma.2004.10.008`.

[2] Y. Bazilevs, V.M. Calo, J.A. Cotrell, J.A. Evans, S. Lipton, T.J.R. Hughes, M.A. Scott, T.W. Sederberg, “Isogeometric analysis using T-splines”, *Computer Methods in Applied Mechanics and Engineering*, 199: 229–263, 2010.

[3] J. Kiendl, K.U. Bletzinger, J. Linhard, R. Wüchner, “Isogeometric shell analysis with Kirchhoff-Love elements”, *Computer Methods in Applied Mechanics and Engineering*, 198(49-52): 3902–3914, Nov. 2009, ISSN 00457825, URL `http://dx.doi.org/10.1016/j.cma.2009.08.013`.

[4] D. Benson, Y. Bazilevs, M. Hsu, T. Hughes, “Isogeometric shell analysis: The Reissner-Mindlin shell”, *Computer Methods in Applied Mechanics and Engineering*, 199(5-8): 276–289, Jan. 2010, ISSN 00457825, URL `http://dx.doi.org/10.1016/j.cma.2009.05.011`.

[5] D. Benson, Y. Bazilevs, M.C. Hsu, T. Hughes, “A large deformation, rotation-free, isogeometric shell”, *Computer Methods in Applied Mechanics and Engineering*, 200(13-16): 1367–1378, Mar. 2011, ISSN 00457825, URL `http://dx.doi.org/10.1016/j.cma.2010.12.003`.

[6] F. Cirak, M. Ortiz, P. Schröder, “Subdivision surfaces: a new paradigm for thin-shell finite-element analysis”, *International Journal for Numerical Methods in Engineering*, 47(12): 2039–2072, Apr. 2000, ISSN 0029-5981, URL `http://doi.wiley.com/10.1002/\%28SICI\%291097-0207\%2820000430\%2947\%% 3A12\%3C2039\%3A\%3AAID-NME872\%3E3.0.CO\%3B2-1`.

[7] Q. Long, P. Burkhard Bornemann, F. Cirak, “Shear-flexible subdivision shells”, *International Journal for Numerical Methods in Engineering*, page n/a, Apr. 2012, ISSN 00295981, URL `http://doi.wiley.com/10.1002/nme.3368`.

[8] S. Balay, K. Buschelman, W.D. Gropp, D. Kaushik, M.G. Knepley, L.C. McInnes, B.F. Smith, H. Zhang, “PETSc Web page”, 2010, http://www.mcs.anl.gov/petsc.

[9] S. Balay, K. Buschelman, V. Eijkhout, W.D. Gropp, D. Kaushik, M.G. Knepley, L.C. McInnes, B.F. Smith, H. Zhang, “PETSc Users Manual”, Technical Report ANL-95/11 - Revision 3.0.0, Argonne National Laboratory, 2008.

[10] L. Piegl, W. Tiller, *The NURBS Book*, Monographs in Visual Communication. Springer, New York, 1995.

[11] G. Farin, *Curves and Surfaces for CAGD: A Practical Guide*, Morgan Kaufmann, 5th edition, 2002.

[12] J.A. Cottrell, T.J.R. Hughes, Y. Bazilevs, *Isogeometric Analysis: Toward Unification of CAD and FEA*, John Wiley and Sons, 2009.

[13] V.V. Novozhilov, *The Theory of Thin Shells*, P. Noordhoff, Ltd. Groningen, The Netherlands, 1959.

[14] A.H. Niemi, J. Pitkäranta, "Bilinear finite element for shells: isoparametric quadrilaterals", *International Journal for Numerical Methods in Engineering*, 75: 212–240, 2008.

[15] A.H. Niemi, "A bilinear shell element based on a refined shallow shell model", *International Journal for Numerical Methods in Engineering*, 81: 485–512, 2010.